PHYSICAL REVIEW B **81**, 205407 (2010)

Bulk Fermi surface coexistence with Dirac surface state in Bi_2Se_3: A comparison of photoemission and Shubnikov–de Haas measurements

James G. Analytis,[1,2] Jiun-Haw Chu,[1,2] Yulin Chen,[1,2] Felipe Corredor,[1,2] Ross D. McDonald,[3] Z. X. Shen,[1,2] and Ian R. Fisher[1,2]

[1]*Stanford Institute for Materials and Energy Sciences, SLAC National Accelerator Laboratory, 2575 Sand Hill Road, Menlo Park, California 94025, USA*

[2]*Geballe Laboratory for Advanced Materials and Department of Applied Physics, Stanford University, Stanford, California 94305, USA*

[3]*Los Alamos National Laboratory, Los Alamos, New Mexico 87545, USA*

(Received 2 February 2010; published 5 May 2010)

Shubnikov-de Haas (SdH) oscillations and angle-resolved photoemission spectroscopy (ARPES) are used to probe the Fermi surface of single crystals of Bi_2Se_3. We find that SdH and ARPES probes quantitatively agree on measurements of the effective mass and bulk band dispersion. In high carrier density samples, the two probes also agree in the exact position of the Fermi level E_F, but for lower carrier density samples discrepancies emerge in the position of E_F. In particular, SdH reveals a bulk three-dimensional Fermi surface for samples with carrier densities as low as 10^{17} cm^{-3}. We suggest a simple mechanism to explain these differences and discuss consequences for existing and future transport studies of topological insulators.

DOI: 10.1103/PhysRevB.81.205407 PACS number(s): 72.20.My, 03.65.Vf, 71.70.Di, 73.25.+i

Recently, a new state of matter, known as a topological insulator, has been predicted to exist in a number of materials: $Bi_{1-x}Sb_x$, Bi_2Se_3, Bi_2Te_3, and Sb_2Te_3.[1,2] This state of matter is characterized by a full band gap in the bulk of the material, but with a gapless, dissipationless surface state. The surface state is comprised of counter-propagating spin states, which create a dispersion of a single, massless Dirac cone that is protected by time-reversal symmetry. The experimental realization of this state could mean significant advances in spintronic devices, quantum computation, and much more besides.

As a result there has been great excitement in the last year after the discoveries of various angle-resolved photoemission spectroscopy (ARPES) experiments[3–5] and more recently from scanning-tunneling measurements[6–8] that such a state appears to exist in nature. Amidst this flurry of recent results, it is easy to forget that these same materials have been the subject of careful and thorough research for much of the 20th century. However, common to all the unambiguous measurements of the Dirac cone is the use of surface-sensitive probes. Only recently have transport measurements emerged specifically investigating the surface state (Refs. 9–11), all of which note the dominance of the bulk conductivity. It is thus of great interest to perform a coordinated study of these materials using both bulk transport experiments and surface sensitive ARPES experiments. Here we report results of these investigations. The transport experiments reveal quantum oscillations that indicate a bulk Fermi surface volume that monotonically changes with carrier density. For carrier densities in the range $\sim 10^{19}$ cm^{-3}, the transport extracted band structure is in quantitative agreement with the bulk band structure determined by ARPES which also observes the Dirac dispersion of the surface state. The quantitative agreement between ARPES and SdH provides additional support for the existence of novel band structure in these materials. For lower carrier density samples down to 10^{17} cm^{-3} we observe SdH oscillations which unambiguously pin the Fermi level in the bulk conduction band, with a high level of consistency across all samples measured from the same batch. While ARPES places E_F near the SdH level for some samples, there are others from the same batch whose E_F is found to reside into the bulk gap. We discuss possible explanations for these discrepancies and the implications for transport studies of surface Dirac fermions in samples near a metal-insulator transition.

The material Bi_2Se_3 can be grown without the introduction of foreign dopants as either n or p type[12,13] though is more commonly found as the former because the dominant defects tend to be Se vacancies. Quantum oscillatory phenomena, which provides evidence of bulk metallic behavior has been reported by Köhler[12] on low carrier density samples and more recently by Kulbachinskii[14] on high carrier density samples. Below a carrier density of 7×10^{18} cm^{-3}, the band structure is well approximated by a single parabolic band, making the interpretation of transport measurements transparent.[14] Two n-type samples with carrier densities differing by 2 orders of magnitude are shown in Fig. 1. For the low carrier density samples an upturn in the resistivity is seen, which levels off at sufficiently low temperature. This behavior has been attributed to the presence of an impurity band whose thermally activated conductivity is comparable to the band conductivity until carriers freeze out at around 30 K.[13,14] This behavior is not apparent in the higher carrier density materials, where the band conductivity always dominates. Furthermore, the mobility increases as the carrier density decreases, consistent with previous measurements.[14] The carrier densities of our highest mobility samples are around an order of magnitude smaller than those of reported topological insulators including Sn-doped Bi_2Te_3($n_e \sim 1.7\times10^{18}$ cm^{-3}) (Ref. 4) or Ca-doped Bi_2Se_3($n_e \sim 5\times10^{18}$ cm^{-3}) (Ref. 5) and as a result may be better candidates in which to observe the transport properties dominated by the topological surface state.

Single crystals of Bi_2Se_3 have been grown by slow cooling a binary melt. Elemental Bi and Se were mixed in alumina crucibles in a molar ratio of 35:65 for batch S1 (n_e

 ©2010 The American Physical Society

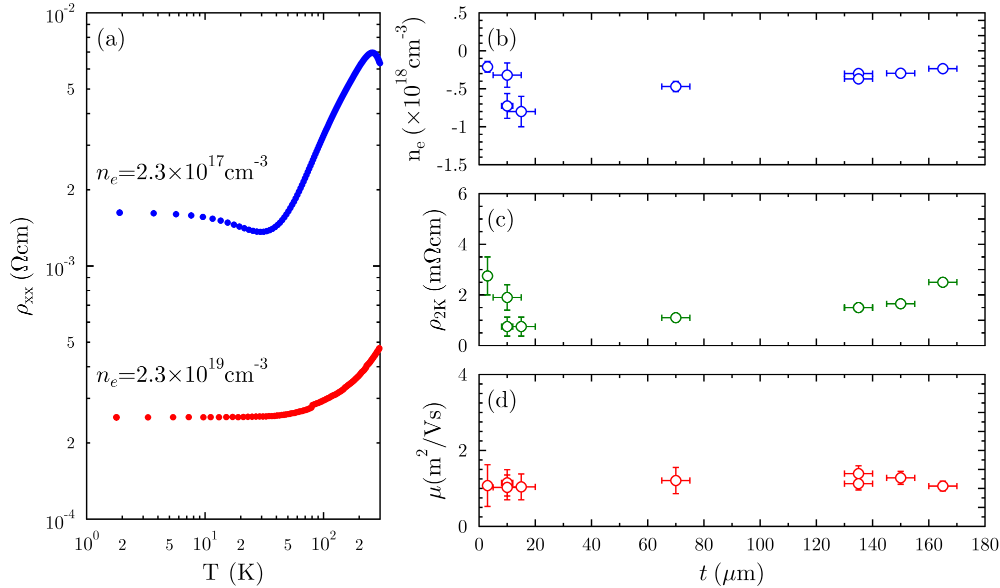

FIG. 1. (Color online) (a) Temperature dependence of two typical samples of Bi_2Se_3 with carrier densities differing by 2 orders of magnitude. (b) Shows the carrier density n_e, (c) the resistivity ρ_0 at T=2 K, and (d) the mobility for samples of different thicknesses. Each sample was a cleave from a parent sample, so that the surface area of each sample was kept constant.

$=5\times10^{17}$), 34:66 for batch S2 ($n_e=3\times10^{17}$), 34:66 for batch S3 ($n_e=2.3\times10^{17}$), and 40:60 for batch S4 ($n_e=2.3\times10^{19}$). The mixtures were sealed in quartz ampules and raised to 750 °C and cooled slowly to 550 °C, then annealed for an extended period. Crystals can be cleaved very easily perpendicular to the (0 0 1) axis. Measurements of the resistivity and Hall effect were measured in a 14 T PPMS using a standard four-probe contact configuration and Hall measurements were performed using a six-probe configuration. For the latter, only data which were linear in the low-field limit were used to avoid mixing with longitudinal components. In addition to this precaution, signal from positive and negative field sweeps was subtracted to extract the odd (Hall) components of the signal, after which the carrier density is extracted in the usual way. ARPES measurements were performed at beam line 10.0.1 of the Advanced Light Source (ALS) at Lawrence Berkeley National Laboratory. Measurement pressure was kept $<3\times10^{-11}$ Torr, and data were recorded by Scienta R4000 analyzers at 15 K sample temperature. The total convolved energy and angle resolutions were 16 meV and 0.2° [i.e., <0.007 (Å^{-1}) or <0.012(1 Å^{-1}) for photoelectrons generated by 48 eV photons], at which energy the cross-section for both surface state and bulk bands is strong.

In Fig. 2 we show complimentary ARPES and SdH data on samples from the same batch with carrier density determined by the Hall effect of $n_e=2.3\times10^{19}$ cm^{-3}. The SdH reveals an anisotropic pocket of frequency 155 T, corresponding to a Fermi energy of around 155 meV above the bottom of the conduction band (the band structure is not parabolic at this filling and so we assume similar band-structure parameters as Köhler[12] characterizing similar carrier density samples of Bi_2Se_3). ARPES results on samples from the same batch show the Fermi level 150 meV above the bottom of the conduction band in good quantitative agreement. Similarly, the effective mass (see below) extracted from SdH is in good quantitative agreement with that measured by ARPES.

In Fig. 3 we illustrate angle-dependent SdH data (a) taken at 1.8 K, on a sample from batch S1 with a lower carrier density of 10^{17} cm^{-3}. The SdH signal reveals a pocket that is approximately an ellipsoid elongated about the $c3$ axis, consistent with measurements by Köhler from the 1970s (Ref. 12) on samples with similar carrier densities. For a two-dimensional pocket expected from the surface state, quantum oscillations should vary as $1/\cos\theta$, where θ is the angle between the $c3$ axis and the field direction, so the present observations must originate from a three-dimensional (3D) Fermi surface existing in the bulk. It has been shown by

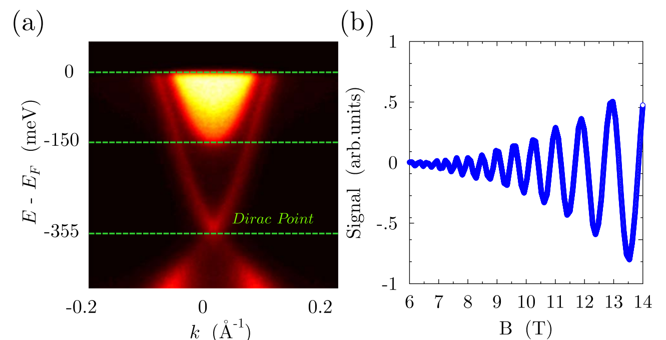

FIG. 2. (Color online) (a) ARPES band dispersion on samples of Bi_2Se_3 with carrier density 2.3×10^{19} cm^{-3} (batch S4). Green lines mark the Fermi level, the bottom of the conduction band, $E-E_F$ $=-150$ meV and the Dirac point, $E-E_F=-355$ meV. (b) Due to the quantization of the energy spectrum into Landau levels, oscillations appear in the magnetoresistance known as SdH oscillations. The SdH oscillations here are for a sample taken from the same batch as in (a) at $\theta=0$, corresponding to a oscillatory frequency of $F=155$ T, consistent with $E_F\sim160$ meV. ARPES and SdH are in good agreement for these high carrier density samples.

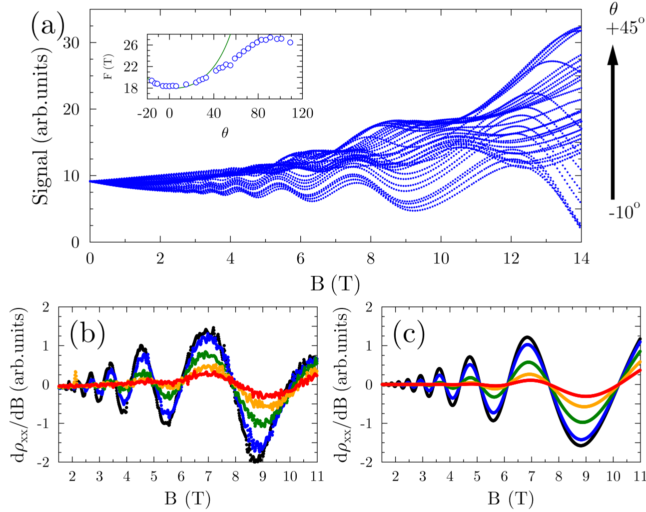

FIG. 3. (Color online) (a) Magnetotransport for samples from S1. As the angle is swept the frequency of the oscillation varies according to the topology of the Fermi surface. For a two-dimensional pocket the expected dependence is $1/\cos\theta$ (shown in green in the inset). The observed angle dependence is clear evidence for a closed ellipsoidal Fermi surface pocket, similar to that observed by Köhler (Ref. 12). Similar SdH data were gathered on batches S2 and S3 on a number of samples. Samples from batch S3 showing the temperature dependence of the derivative of the SdH signal in (b) and a fit to the data shown in (c) from which the effective mass, Dingle temperature, and oscillatory frequency can be extracted.

Köhler[12] and more recently by Kulbachinskii *et al.*[14] that the conduction-band structure for these low carrier densities is approximately parabolic, and so the band filling can be estimated by $E_F=\frac{\hbar^2 A_k}{2\pi m^*}$, where A_k is the area of the Fermi surface in Fourier space. The Shubnikov-de Haas frequency is ~18 T corresponding to a Fermi energy of 17 meV above the bottom of the conduction band.

In Fig. 3(b) we show the derivative of the longitudinal magnetoresistance of a sample from batch S3 and a fit of the entire data set using the usual Lifshitz-Kosevich formalism,[15] to extract the effective mass and Dingle temperature T_D, with fit shown in Fig. 3(c). Fitting the entire data set, which is often more accurate than tracing the amplitude of the Fourier transform, our fit yields $m^*=0.15m_e$ and $T_D=3.5$ K, for this frequency ($F=14$ T). Similar data for samples from batch S4 give $m^*=0.125m_e$, $T_D=4$ K, and $F=155$ T. The mean free path is calculated using the orbitally averaged velocity and scattering time extracted from T_D yields $l_{S3}\sim 60$ nm and $l_{S4}\sim 220$ nm. These data are wholly consistent with the very complete SdH studies of Köhler *et al.*[12,13] and more recently by Kulbachinskii *et al.*[14] In addition, the data were reproduced with high consistency on a number of samples from the same batch, and even on samples from different batches with similar growth parameters.

ARPES data on samples from the same batches as those shown in Fig. 3 determine the effective mass to be $m^* \sim 0.13m_e$ in very good quantitative agreement with SdH. However, the exact placement of the Fermi level in the band structure reveals some disagreement. In Fig. 4 we illustrate

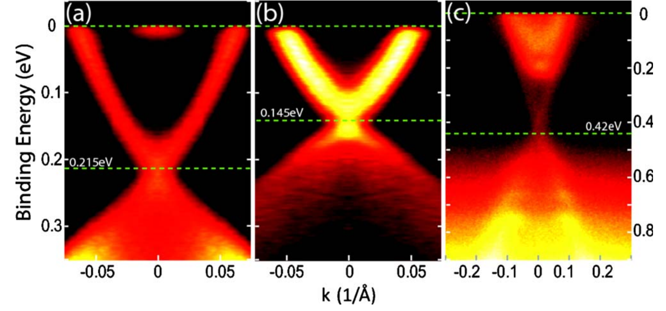

FIG. 4. (Color online) ARPES data on samples of Bi_2Se_3 from batch S1. The horizontal lines show the crossing of the Fermi level ($E-E_F=0$) and the Dirac crossing. (a) Band structure measured by ARPES results on samples from batch S1 showed the Fermi level near the SdH level of ~17 meV from the bottom of the conduction band. (b) Measurement on another sample from batch S1 showed the Fermi level in gap. Some other samples from S2 and S3 also showed the Fermi level in the bulk gap. The variation might be due to the lower carrier density of these samples, and the surface band structure is more susceptible to small amounts of surface contamination. (c) Band structure of a sample also from batch S1 which was cleaved in atmosphere and exposed for 10 s, showing significant *n*-type doping with large bulk conduction-band pocket.

photoemission data for two separate samples from batch S1. In Fig. 4(a) the Fermi level is near the bottom of the conduction band in agreement with SdH while in Fig. 4(b) it is in the gap (about 60 meV below the conduction band), crossing the Dirac cone with apparently no bulk contribution. A number of samples from similar batches, such as batches S2 and S3, also have shown similar variation in E_F crossing the gap on some samples. Table I summarizes typical values of the Fermi energy determined by SdH and ARPES. E_F determined by photoemission is up to 75 meV below the SdH Fermi level, and we now explore reasons for this discrepancy.

Such differences could occur due to sample variation within a batch, so that samples measured by ARPES are chemically different from those measured by transport. However, the transport from more that 20 samples from batches S1, S2, and S3, the SdH consistently showed E_F to be ~15 meV above the bottom of the conduction band, and so

TABLE I. SdH and ARPES determined Fermi energies E_F and conduction-band effective masses for various batches. Values of E_F are given relative to the bottom of the conduction band.

	SdH		ARPES	
Batch	E_F (meV)	$m^*(m_e)$	E_F (meV)	$m^*(m_e)$
S1	17(2)	0.15(2)	10(5)	0.13(2)
S1	17(2)	0.13(2)	−60(10)	n/a
S2	14(2)	0.13(2)	−75(10)	n/a
S3	14(2)	0.13(2)	5(5)	0.13(2)
S3	14(2)	0.13(2)	−10(10)	n/a
S4	160(5)	0.125(5)	150(10)	0.13(2)

sample dependence seems unlikely. Another reason for the discrepancy may be that atmospheric exposure of transport samples has contaminated them with an n-type dopant causing them to appear bulk n type. Figure 4(c) illustrates photoemission data for a sample cleaved in air. The Dirac cone of the surface state remains robust and the bulk conduction band appears partially occupied. Such doping may lead to a 3D Fermi surface pocket appearing in SdH oscillations if the contamination is deep enough and allows for sufficiently long mean free paths.

To investigate this possibility further we measure the thickness dependence of the transport by systematically thinning a single sample. Cleaving was achieved with tape, keeping the cross-sectional area of the resulting samples relatively constant and allowing direct comparison of data sets of each cleave. Though the samples are vulnerable to deformations between cleaves, only data from mirrorlike flat samples are presented. In most cases these samples still exhibited quantum oscillatory phenomena, confirming the high quality of the cleaved samples. Figures 1(b)–1(d) show a summary of the low-temperature carrier density, resistivity, and mobility as a function of thickness. Within our error bars, each quantity seems to vary weakly down to 3 μm in thickness. Although the residual resistivity and carrier density vary slightly (possibly from disorder related to slight sample deformation, despite the precautions mentioned above), the mobility remains almost constant as a function of thickness at $\mu \sim 1\ \mathrm{m}^2/\mathrm{V\ s}$. In summary, the transport is insensitive to the thickness, suggesting that the SdH oscillations are not a consequence of atmospheric contamination, but originate from the intrinsic band conductivity of the bulk.

A final scenario for the discrepancy is that the band structure is distorted near the surface due to space-charge accumulation. This is known to occur in many semiconductors, such as InSb or CdTe,[16,17] whereby the bulk band structure bends as the surface is approached. Typically, such bending occurs over a surface depletion layer z_d, which can be calculated by solving the Poisson equation to yield $z_d^2 = \kappa\epsilon_0 \Delta V / e n_e$,[18] where κ is the dc dielectric permittivity [estimated from these samples as ~ 113 (Ref. 19)] and ΔV is the difference in energy between the surface and bulk states. We estimate $z_d^{S1} \sim 40$ nm for the low carrier density samples and $z_d^{S4} \sim 2$ nm for the high carrier density samples. A schematic representation of the band bending is shown in Fig. 5. The present argument suggests that discrepancies between ARPES and SdH can be explained, even expected for low carrier density samples. In addition, due to the small value of n, these samples are likely more susceptible to a small amounts of surface contamination, especially if the uncontaminated surface E_F is in the gap (as illustrated in by ARPES on atmosphere exposed samples). This may help explain why there is some variability in the Fermi level of ARPES data but not in the SdH data.

Much theoretical work has emerged on the dramatic consequences of the surface state on transport properties.[20] Yet over several decades of experimental study, such properties have not been observed. Recently, Aharanov-Bohm and universal conductance fluctuations have been observed which may be due to the surface state,[10,11] but even in these cases the conductance appears bulk at the temperatures considered. Conventionally, such intrinsically doped materials can become "insulators" by either a Mott-type or an Anderson transition. The first can occur when the Bohr radius $a_B = \kappa\hbar^2/m^* e^2$ falls below the Thomas-Fermi screening length λ_{TF}, so that wave functions cannot overlap. This can be estimated using $\lambda_{TF}^2 = \kappa\epsilon_0/[2\pi e^2 g(E_F)]$, where $g(E_F)$ is the number of states per unit volume per unit energy, estimated by Middendorff *et al.*[21] In the present case, the large κ and small m^* tend to make a_B very large. For the lowest carrier density samples investigated here $a_B \sim 3$ nm and $\lambda_{TF} \sim 4$ nm, which places this material on the metal-insulator boundary. The carrier density can also be reduced by introducing foreign dopants which "drain" the excess carriers and pin the chemical potential μ in the gap. For hydrogeniclike impurities this can be very effective, but in the present materials impurity bands often form instead. At high-enough impurity densities the carriers may become Anderson localized. Such samples are characterized by a high carrier density with very low mobility, leading to a negative gradient in the temperature dependence of the resistivity. This may be the case, for example, in $Bi_xSb_yPb_zSe_3$ which has $\rho \sim 30\ \mathrm{m}\Omega\ \mathrm{cm}$ yet a carrier density $n_e \sim 5 \times 10^{18}\ \mathrm{cm}^{-3}$ (Ref. 22)—a value similar to that of recently reported topological insulators.[3–5] An Anderson insulator is generally bad news for topological insulators, because even though at zero temperature the bulk conductivity $\sigma = 0$, at finite temperature the transport may remain dominated by bulk hopping mechanisms.

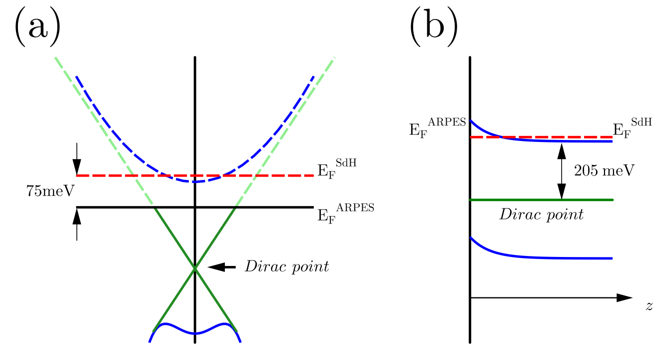

FIG. 5. (Color online) (a) A schematic representation of the band structure seen by ARPES (solid) red horizontal line denoting the Fermi level as seen by SdH. (b) We infer band bending of about 75 meV at the surface from a comparison of ARPES (Fig. 4) and quantum oscillations (Fig. 3).

In conclusion, the present study reveals substantial agreement between transport and ARPES measurements of the fermiology of Bi_2Se_3, in particular, for samples with large carrier densities. However, for samples with carrier densities approaching $10^{17}\ \mathrm{cm}^{-3}$, discrepancies emerge as to the exact position of the Fermi level. We have confirmed the bulk nature of the transport by the thickness dependence of the Hall effect, resistivity, and mobility. Furthermore SdH data are highly consistent between different samples from the same batch. Interestingly, the carrier densities measured here are

an order of magnitude smaller than those of the topological insulators recently reported in the literature.[3,4,10,11] ARPES and scanning tunneling microscope have been invaluable tools in revealing the physics of topological insulators, providing compelling evidence for the presence of the topologically protected Dirac surface state. The present results should stimulate further theoretical work as to the consequences of the coexistence of bulk and surface states in a single sample as well as innovation in novel ways to fabricate these materials so the bulk state can be cleanly eliminated.

We would like to thank D. Goldhaber-Gordon, J. R. Williams, X. Qi, S.-C. Zhang, K. Lai, J. Koralek, J. Orenstein, and T. Geballe for useful discussions. Work was supported by the U.S. DOE, Office of Basic Energy Sciences, under Contract No. DE-AC02-76SF00515.

[1] J. C. Y. Teo, L. Fu, and C. L. Kane, Phys. Rev. B **78**, 045426 (2008).
[2] H. Zhang, C. Liu, X. Qi, X. Dai, Z. Fang, and S. Zhang, Nat. Phys. **5**, 438 (2009).
[3] D. Hsieh *et al.*, Science **323**, 919 (2009).
[4] Y. L. Chen *et al.*, Science **325**, 178 (2009).
[5] D. Hsieh *et al.*, Nature (London) **460**, 1101 (2009).
[6] Z. Alpichshev, J. G. Analytis, J. H. Chu, I. R. Fisher, Y. L. Chen, Z. X. Shen, A. Fang, and A. Kapitulnik, Phys. Rev. Lett. **104**, 016401 (2010).
[7] P. Roushan, J. Seo, C. V. Parker, Y. S. Hor, D. Hsieh, D. Qian, A. Richardella, M. Z. Hasan, R. J. Cava, and A. Yazdani, Nature (London) **460**, 1106 (2009).
[8] K. Gomes, W. Ko, W. Mar, Y. Chen, Z. Shen, and H. Manoharan, arXiv:0909.0921 (unpublished).
[9] A. A. Taskin and Y. Ando, Phys. Rev. B **80**, 085303 (2009).
[10] J. G. Checkelsky, Y. S. Hor, M. H. Liu, D. X. Qu, R. J. Cava, and N. P. Ong, Phys. Rev. Lett. **103**, 246601 (2009).
[11] H. Peng, K. Lai, D. Kong, S. Meister, Y. Chen, X.-L. Qi, S.-C. Zhang, Z.-X. Shen, and Y. Cui, Nature Mater. **9**, 225 (2010).
[12] H. Köhler, Phys. Status Solidi B **58**, 91 (1973).
[13] H. Köhler and A. Fabbicius, Phys. Status Solidi B **71**, 487 (1975).
[14] V. A. Kulbachinskii, N. Miura, H. Nakagawa, H. Arimoto, T. Ikaida, P. Lostak, and C. Drasar, Phys. Rev. B **59**, 15733 (1999).
[15] D. Schoenberg, *Magnetic Oscillations in Metals* (Cambridge University Press, London, 1984).
[16] P. D. C. King, T. D. Veal, M. J. Lowe, and C. F. McConville, J. Appl. Phys. **104**, 083709 (2008).
[17] R. K. Swank, Phys. Rev. **153**, 844 (1967).
[18] W. Monch, *Semiconductor Surfaces and Interfaces* (Springer, New York, 2001).
[19] U. R. O. Madelung and M. Schulz, *Non-Tetrahedrally Bonded Elements and Binary Compounds I* (Springer, 1998), pp. 1–12.
[20] D. H. Lee, Phys. Rev. Lett. **103**, 196804 (2009).
[21] A. Middendorff, H. Kohler, and G. Landwehr, Phys. Status Solidi B **57**, 203 (1973).
[22] J. Kašparová, C. Drasar, A. Krejcova, L. Benes, P. Lost'ak, W. Chen, Z. Zhou, and C. Uher, J. Appl. Phys. **97**, 103720 (2005).